Sādhanā (2020)45:12
https://doi.org/10.1007/s12046-019-1246-2

Experimental investigations on transient cryogenic chilldown of a short horizontal copper transfer line

JESNA MOHAMMED[1,*], ABDUL MOHIZIN[2] and K E REBY ROY[1]

[1]Department of Mechanical Engineering, TKM College of Engineering, Kollam 691005, India
[2]Department of Mechanical Engineering, Graduate School, Kookmin University, Seoul 02707, Republic of Korea
e-mail: jesnamohammed@tkmce.ac.in; amohizin@kookmin.ac.kr; rebyroy@tkmce.ac.in

MS received 6 March 2018; revised 11 November 2019; accepted 18 November 2019

Abstract. The present study investigates chilldown characteristics of a horizontal copper transfer line with 7.94 mm outer diameter, 0.81 mm wall thickness and 500 mm length. Data presented in this paper is for the experiments conducted with different mass fluxes (66 kg $(m^2.s)^{-1}$ to 102 kg $(m^2.s)^{-1}$) in a horizontal copper transfer line under terrestrial gravity conditions. Temperature measurements were recorded at six equidistant points to a distance of 330 mm from an inlet. Inverse problem solving method is utilized to calculate corresponding heat flux and heat transfer coefficients. Considering the thermal properties of the quenched wall, an empirical relation was developed. It is found that while employing copper transfer lines instead of stainless steel, thermal mass of the section is reduced by a factor of 100, thereby encountering a reduction of 50% in critical heat flux.

Keywords. Chilldown; liquid nitrogen boiling; flow boiling; critical heat flux; Leidenfrost point; minimum heat flux.

1. Introduction

The journey of food particles has to be closely monitored from harvest to table in order to conserve its element of freshness. This calls for an economic and effective preservation technique. Cryo-freezing is gaining popularity among the food industries as an effective method of preservation technique. It offers good retention of original quality making processed food indistinguishable from original raw material in terms of quality. Among cryogenic liquids, (LN2) has a tremendous potential to be used as a total loss refrigerant and find applicability in different aspects of food processing and preservation [1, 2]. Transport of LN2 and other cryogens is an indispensable process during these preservation techniques. A complicated process involving unsteady two-phase heat and mass transfer precedes a normal operating system where, to have the cryogen in liquid form, the transfer lines has to be brought from ambient temperature to a desirable steady cryogenic temperature. Predicting the accurate chilldown time and heat flux associated with it is extremely important in many of these applications as, like every other refrigeration technique the quality of the preserved food depends upon the refrigeration rate.

Intricate interaction between the two-phase flow and boiling heat transfer increases the complexity of the chilldown process. When certain physical properties like lower surface tension, very low latent heat, near zero wetting angle and large ratio of vapour density to liquid density, are taken into account, most of the current empirical and semi-empirical correlations and research findings for heat and mass transfer would break down under cryogenic conditions. Chilldown in transfer lines are mainly affected by mass flow rate, initial wall superheat, liquid subcooling, gravity, material properties and orientation of the tube. Research is still going on in analysing the effects of various factors in this process. Difficulties in setting up experiments with cryogenic fluids provide little data in chilldown of cryogenic fluids. Investigations in this field dates back to decades and began in the early 1960s with the advent of cryogenic fluids in aerospace applications. Some of the notable works were of Burke *et al* [3], Bronson *et al* [4], and Chi [5]. Burke *et al* [3] in 1960 experimentally investigated the chilldown process in a pressurized horizontal pipe using liquid nitrogen as test fluid. He predicted the existence of single phase convective heat transfer and film boiling. Bronson *et al* [4] in 1962 conducted visual studies on horizontal pipelines in order to study the flow structures present in two-phase flow of liquid hydrogen (LH2). He pointed out the existence of circumferential temperature variations and the occurrence of flow stratification during LH2 chilldown. In an

Jesna Mohammed and Abdul Mohizin contributed equally.

*For correspondence
Published online: 03 January 2020

experimental investigation of chilldown of copper test sections employing liquid hydrogen by Chi and Vetere [5] in 1963, slug flow appeared upon the chill down process. Their primary focus was on identifying the flow regime transitions by correlating visual observations with transient wall temperature measurements. Later in 1965 Chi [6] used liquid hydrogen for studying chilldown of aluminium transfer lines. His observations showed that 90% of chilldown time was occupied by film boiling. Based on his observations, boiling regimes of single phase convective boiling, film boiling and nucleate boiling were established. In 1974 Srinivasan *et al* [7] studied chilldown mechanism in short transfer lines made of copper, aluminium, glass and stainless steel and concluded that mass flow rate does not have a significant effect in chilldown time for short transfer lines. However studies by Chi [6], Yuan *et al*. [8, 9], Jackson *et al* [10], Hu *et al* [11] showed a reduction in chilldown time with increase in mass flux. Jackson *et al* [12] in 2005 provided a procedure for predicting the transient heat transfer coefficient in a horizontal transfer line. Yuan *et al* [8, 9] provided chilldown of cryogenic systems under low flow rates in 2007 and later in 2009 proposed a Numerical modelling procedure in terrestrial and microgravity conditions. Yuan *et al* [8] correlated the visual observations with circumferential temperature gradients and suggested that the liquid filament-wall interaction was the major contributor to the chilling of bottom wall of transfer line whereas forced convection of superheated vapour prevailed on the upper wall of transfer line.

Recent years has witnessed an upraised interest among the research community and resulted in extensive studies in this direction. In 2012 Hu *et al* [11] conducted experiments to study the effect of flow patterns created during high and low mass fluxes and analyzed heat flux, chilldown time for flow in the upward and downward direction through a vertical pipe. They observed that the total chilldown time for upward flow was longer than that of downward flow and critical heat flux was higher in downward flow condition. Shaeffer *et al* [13] investigated the chilldown effect in LN2 transfer lines. They studied the effect of varying mass flux or Reynolds number in pulsating and continuous flow. From their findings, it is evident that chilldown time is less for continuous flow where 95% of the time consumption is in the film boiling region. They also proposed that film boiling region have the lowest chilldown efficiency, as low as 5–8% whereas, the nucleate boiling region has the highest chilldown efficiency.

A CFD simulation of liquid pool boiling was made by Liu *et al* [14] in 2015. Their study was focused on the effects of changing ground temperature on vaporization rate of cryogenic liquid. A comparison of cryogenic flow boiling between liquid nitrogen and liquid hydrogen was done by Hartwig *et al* [15]. Experiments with high and low Reynolds numbers were performed and it was concluded that chilldown occurs more rapidly at higher Reynolds numbers due to quick transition from vapor flow to annular liquid flow. It was observed that liquid hydrogen chilldown proceed immediately into nucleate boiling regime at higher Reynolds numbers compared to liquid nitrogen. They also noted that, 75% of chilldown time was spent in film boiling regime.

Johnson *et al* [16] made experimental and numerical studies of chilldown of horizontal and inclined pipes in 2015. Their major focus was on predicting the local heat transfer coefficient and heat flux for a transient chilldown period using an inverse heat transfer technique. They observed low variation in chilldown time for inclination up to 10°. Darr *et al* [17, 18] in 2016 published a two-part series of papers which discusses the experimental results of parametric effects of mass flux, inlet subcooling, equilibrium quality, pressure and flow direction with respect to gravity in liquid nitrogen chilldown tests of a stainless steel tube. Based on the observations from data points, they developed a correlation to predict the heat transfer coefficients for a cryogenic chilldown process in a straight transfer line.

Majority of the reported works were on stainless steel or pyrex glass test sections in vacuum insulated conditions. Very few data on chilldown in copper transfer lines are available. OFHC copper tubes are commonly used in cryogenic systems because it remains ductile at low temperature. Copper tubes possess an advent of added flexibility in transfer lines but the increased parasitic heat influx due to high thermal conductivity limits its practicability in cryogenic systems and so are the studies on copper transfer lines. As far as heat transfer is concerned, the vast majority of 'insulation' on an uninsulated line is the convective heat transfer coefficient between the pipe and air, it can be further minimized by adding a light insulation (PUF), so the high thermal conductivity of the pipe material may not be decisive. In this work, a study of copper transfer lines with simple insulation such as Polyurethane foam insulation is attempted and similar chilldown trends in previous literatures were observed.

2. Experimental set-up

A schematic layout of the experimental setup is shown in figure 1. The entire setup consists of three sections, namely:

- liquid nitrogen storage and supply system
- test section
- instrumentation and data acquisition system.

Liquid nitrogen possesses many desirable characteristics like non-corrosiveness, chemical inertness, ease of availability, non-flammability and cheaper cost and hence a favourite among the research community in chilldown studies. Moreover it does not pose any major health hazards. In the present study, liquid nitrogen was stored in IBP Co. Limited made TA-55, Dewar of capacity 55 L. The liquid nitrogen Dewar was pressurized using gaseous

nitrogen stored in a cylinder of 47 L capacity. The high pressure gaseous nitrogen cylinder can supply gas at a maximum pressure of 15 bar. The liquid nitrogen flow rate was controlled manually by controlling the Dewar pressure with the help of a pressure regulator mounted on the gaseous nitrogen cylinder.

Test section under consideration was 5/16″ OFHC Copper tubes (UNS C10100) of 7.94 mm outer diameter, 0.81 mm wall thickness and 500 mm length and its thermophysical properties are given in appendix. Liquid was supplied to the horizontal transfer line through 1/2″ SS 304 grade pipes and brass fittings. Water vapour and other condensable gases in the system were removed by purging it with gaseous nitrogen prior to the experiment. Initially Valve 2 is closed and Valve 3 and Valve 1 are kept in open position. When a steady flow of liquid nitrogen is observed in the flexible bypass line, and a cut off temperature of 120 K is measured by the temperature sensor mounted on the inlet of Valve 2, Valve 2 was opened and Valve 3 was closed simultaneously. This was used to ensure the entry of single phase liquid nitrogen into the test section.

The heat in-leak to the test section was minimised using polyurethane foam insulation (thermal conductivity of 0.02 (W (m. K)$^{-1}$) having a thickness of 56 mm throughout the test length.

The wall temperature measurements were recorded at six equidistant points up to a distance of 330 mm from inlet by employing T-type thermocouples tied onto the tube surface using a thin copper wire. Outer wall temperature of insulation was also monitored at three equidistant points as shown in figure 2. Keysight 34972A data acquisition/data logger switch unit with a scan frequency of 30 milliseconds was used for data logging. The average mass flux was measured using a volume flow meter having an accuracy of 0.05 mm^3.s^{-1}. It is mounted with a mercury thermometer at the outlet to measure the average temperature of the outgoing gas. To ensure the absence of liquid nitrogen in the flow meter, the exit line from the test section is kept in a hot water bath.

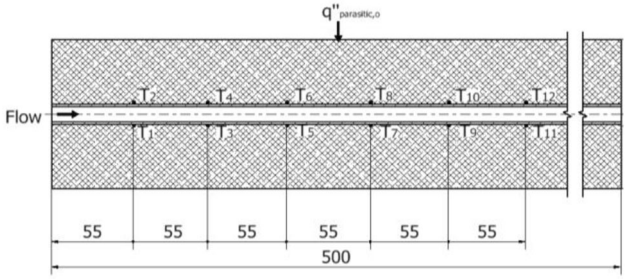

Figure 2. Thermocouple locations on test section. All units are in mm.

The major source of uncertainty in measurements was from the temperature measurement from thermocouples, DAQ and volume flow meter. An uncertainty of ±1 K is to be expected from temperature measurements and a summary of uncertainty is given in table 1. The experiments in each input condition were conducted thrice for ensuring repeatability.

3. Results and discussion

Bottom wall temperature measurement obtained at a distance of 55 mm from the inlet section was compared qualitatively with that reported in literatures [8, 10, 16] using non-dimensional parameters. Non-dimensional temperature T* is the ratio of transient wall temperature to initial wall temperature and non-dimensional time t* was taken as the ratio of elapsed time to chilldown time obtained at that condition. Wall temperature measured by Jackson *et al* [10] and Johnson *et al* [16] was at a distance of 0.150 m and 0.090 m away from the inlet, and they clearly demarked the three different phases of chilldown phenomena, namely:

- Region A: Film boiling regime, where the flow structure can be either dispersed or inverted annular

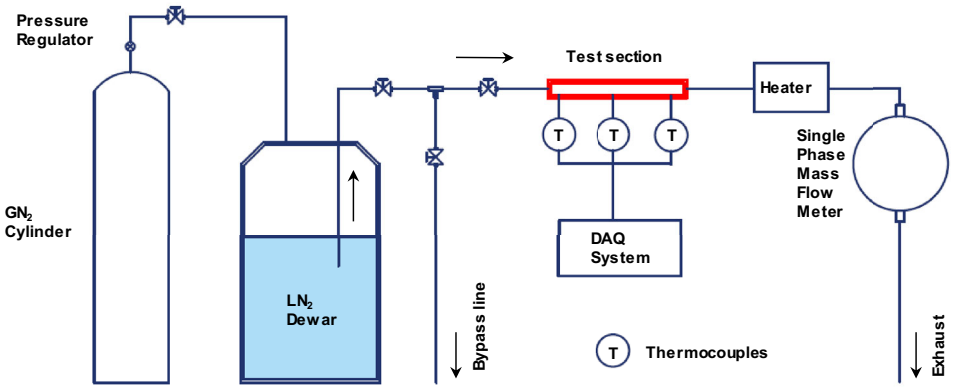

Figure 1. Layout of experimental setup for chilldown studies.

Table 1. Uncertainty summary.

Symbol	Quantity	Units
d	±0.001	m
T	±0.5	K
Volume flow rate	0.05	$mm^3.\ s^{-1}$
Maximum deviation in q″	15.9 %	
Maximum deviation in h_i	13.7%	

film flow. In this region the wall temperature reduces gradually.

- Region B: Transition boiling regime, where a sudden drop in temperature is observed as liquid droplets begin to wet the wall. The sudden drop in wall temperature is due to the wetting of wall surface by liquid droplets.
- Region C: Nucleate boiling regime, where flow can either be bubbly or slug flow. Wall temperature slope is almost zero in this region.

These results were consistent with the present studies when compared with the details in Figure 3.

In the present study, it is observed that the transition temperature of bottom wall at 102 kg $(m^2.s)^{-1}$ at a section z = 0.055 m from inlet, was 133 K with a drop of 15 K in 7 s, whereas it was 137 K with a drop of 16 K in 11 s, for 86 kg $(m^2.s)^{-1}$. For 66 kg $(m^2.s)^{-1}$ it was 127 K with corresponding temperature drop of 12 K in 8 s.

The temperature profile of bottom wall at section 55 mm from inlet at 102 kg $(m^2.s)^{-1}$, 86 kg $(m^2.s)^{-1}$ and 66 kg $(m^2.s)^{-1}$ is illustrated in figure 4. Thus, it can be concluded that the transition from film boiling to nucleate boiling can happen at higher wall temperatures with increase in mass flux and is in agreement with published studies [6, 8, 9, 11, 12, 16].

This phenomenon can be explained as follows. When liquid nitrogen enters the test section, which is in thermal

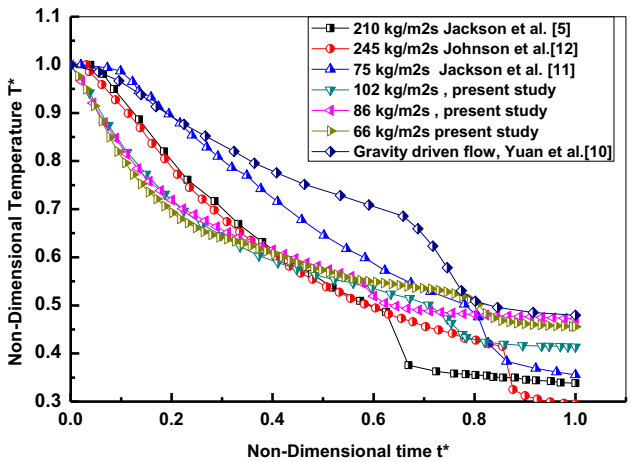

Figure 3. Comparison of results of available literatures with present study.

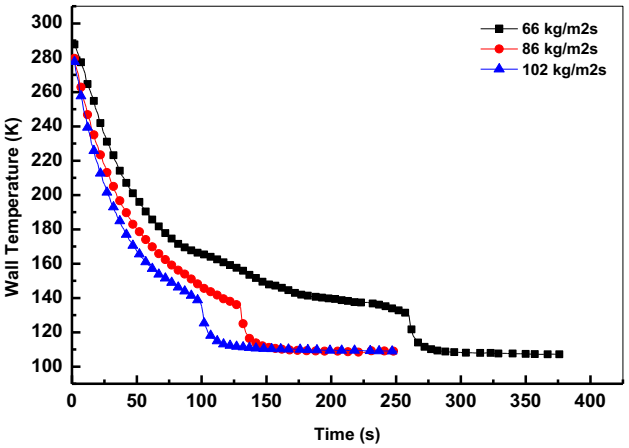

Figure 4. Comparison of bottom wall temperature of straight pipe at section 0.055m from inlet at 102 kg $(m^2.s)^{-1}$, 86 kg $(m^2.s)^{-1}$and 66 kg $(m^2.s)^{-1}$.

equilibrium with the ambient, instant evaporation occurs owing to the high wall superheat. With the passage of time, the wall cools down and reduces the temperature difference, an inverted annular flow regime or dispersed flow may be observed. However in terrestrial gravity condition the liquid core is influenced by the effect of gravity and it tends to wet the lower side of the pipe wall. But, a thin layer of vapor film may be formed by the evaporating liquid which restricts the liquid wall interaction. As the flow rate increases, the liquid core velocity also increases. After a critical point the liquid cores carries away the vaporizing liquid and restrict the formation of vapor film, thereby flooding the bottom wall. At this point, the wall temperature drops rapidly as observed.

3.1 *Inner wall temperature, heat flux and heat transfer coefficient evaluations*

In chilldown studies, inner wall temperature, heat flux and heat transfer coefficients are of particular interest. However in the present study, outer wall temperature measurements were the only direct temperature measurements. In similar studies conducted by Schieffer *et al*[13] and Hu *et al*[11] used Burggraf correlations for the determination of inner wall temperature, T_i and heat flux, q_i''. The method is based on lumped capacitance analysis and can produce accurate results using fewer terms. The model neglects axial heat transfer along the test section.

Inside wall temperature can be given by the correlation

$$T_i = T_0 + \left(\frac{r_0^2}{4\alpha}\left(\left(\frac{r_i}{r_0}\right)^2 - 1 - 2\ln\frac{r_i}{r_0}\right)\right)\frac{dT_0}{dT} + \left(\frac{1}{64\alpha^2}\left(r_i^4 - 5r_0^4\right)\frac{r_0^2 r_i^2}{8\alpha^2}\ln\frac{r_i}{r_0} - \frac{r_0^4}{16\alpha^2}\ln\frac{r_i}{r_0}\frac{r_0^2 r_i^2}{16\alpha^2}\right)\frac{d^2T_0}{dt^2} + \ldots \quad (1)$$

And inner wall surface heat flux can be calculated with the equation

$$q_i'' = \rho c\left(\frac{r_i^2 - r_0^2}{r_i}\right)\frac{dT_0}{dt} + \left(\frac{(\rho c)^2}{k}\left(\frac{r_i^3}{16} - \frac{r_0^4}{16r_i} - \frac{r_0^2 r_i}{16}\ln\frac{r_i}{r_0}\right)\right)\frac{d^2T_0}{dt^2} + \frac{(\rho c)^3}{k^2}\left(\frac{r_i^5}{384} - \frac{3r_0^4 r_i}{128} + \frac{3r_0^2 r_i^3}{128} - \frac{r_0^6}{384 r_i} - \frac{r_0^2 r_i^3}{128}\ln\frac{r_i}{r_0} - \frac{r_0^4 r_i}{32}\ln\frac{r_i}{r_0}\right)\frac{d^3T_0}{dt^3} + \cdots \quad (2)$$

The parasitic heat load present through the insulation provided can be calculated as:

$$q''_{\text{parasitic,o}} = q''_{\text{cond,o}} + q''_{\text{conv,o}} + q''_{\text{rad}} \quad (3)$$

As the temperature difference between the surface of the insulation and surrounding was negligible, the convective and radiative heat transfer at the surface of the insulation can be neglected.

$$q''_{\text{cond,o}} = -\left(kA\,\frac{\partial T}{\partial x}\right) \quad (4)$$

Thus,

Net heat transfer at inner wall can be calculated as:

$$q'' = \frac{r_0}{r_i}(q''_{\text{parasitic,o}}) - q_i'' - q_a' \quad (5)$$

In chilldown processes the axial conduction heat transfer, q_a'' is normally considered as negligible [9].

Heat transfer coefficient can be found using the equation

$$h_i = \frac{q''}{(T_i - T_{sat})} \quad (6)$$

Inner wall temperature profile was found to have small or negligible variation from the outer wall profiles. This may be due to the small thickness and high thermal conductivity of the test section. Heat flux is plotted as a function of wall superheat of straight tube at 102 kg $(m^2.s)^{-1}$ in figure 5.

The curve is similar to boiling curve in pool boiling conditions. Critical heat flux and Leidenfrost point were clearly identified. The three regimes of boiling can be distinguished in figure 5 as Film Boiling Regime (A-B), Transition Boiling Regime (B-C) and Nucleate Boiling Regime(C-D).

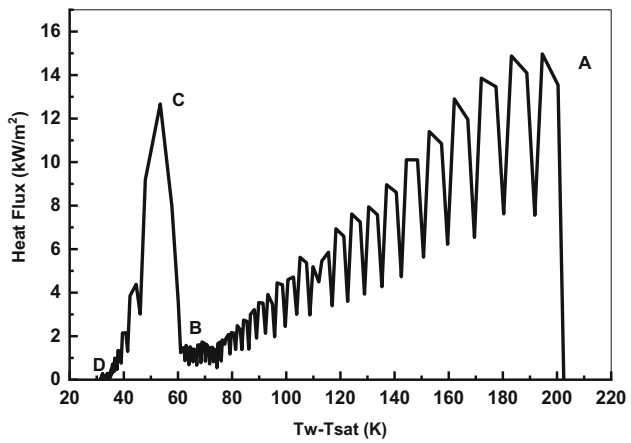

Figure 5. Variation of heat flux with wall superheat.

While solving Eq. (2) there are significant oscillations in the time-derivatives, especially in the second- and third-order terms. Darr *et al* [17, 18] reported that these oscillations occur for all low mass flux tests. In such conditions the chilldown process is so slow, so that any small noise during the temperature measurement process can cause large slope changes. This variation in slope could cause large changes in the second- and third-order numerical derivatives especially at the beginning of the chilldown process. The high wall superheat in the beginning of the process can cause the incoming liquid to vaporize instantaneously and causes a dip in the temperature reading. But, in case of high mass flux flows, large changes in temperature between successive measurements creates a smoother derivatives. Thus, in such cases the effect of small noises becomes negligible. A detailed description on the oscillations of second and third derivatives of Eq. 2 could be found in reference [18].

The computed heat flux and heat transfer coefficient with time is shown in figure 6(a) and (b). The general observations can be summed up as (i) At the beginning of chilldown process heat transfer coefficient is found to be higher for higher mass fluxes and thereby increase in heat flux. (ii) At higher mass fluxes, quenching of pipe wall occurred earlier due to increase in fluid velocity resulting in the earlier occurrence of nucleate boiling. (iii) Critical heat flux is found to be higher for higher mass fluxes.

3.2 *Critical heat flux*

Critical heat flux represents maximum heat flux for the nucleate boiling regime and for a chilldown curve, it represents the onset of nucleate boiling.

Over the past century, various correlations were proposed for the prediction of critical heat flux for pool boiling conditions. Among the proposed works, relations used for predicting CHF in previous literatures [13, 15, 16, 19] were Zuber correlation [20], Leinhard and Dhir [21], Katto *et al* [20–22], Mudawar and Maddox [23] and Darr *et al* [24]. Many literatures used Zuber correlations [20] to find the CHF. Hu *et al* [11] and Yuan *et al* [8] found that the correlation over predicted the measured heat flux and Schieffer *et al* [13] found a 7–12% variation in critical heat flux. Hartwig *et al* [15] used all four correlations and found that all the correlations over predicted the CHF value for LN2 and under predicted the CHF value for LH2, except Katto's group [25–27].

Zuber [20] proposed a model for stationary fluid in pool boiling conditions and is applicable when vapour liquid interface of the escaping vapour becomes unstable due to Helmholtz instability. The proposed model is

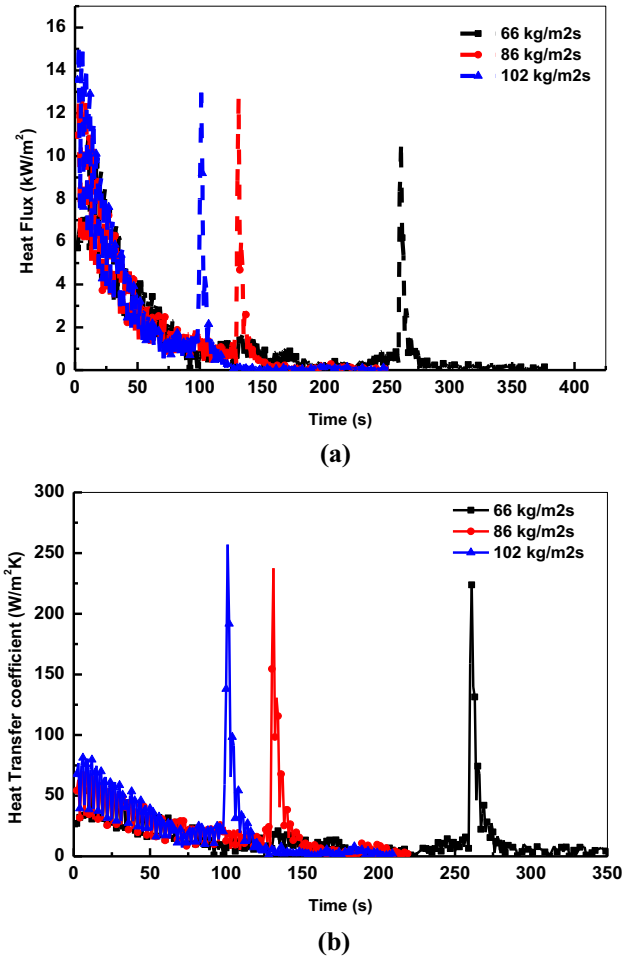

Figure 6. (**a**) Transient characteristics of heat flux, (**b**) inner wall heat transfer coefficient at z = 0.110 m.

$$q''_{CHF} = 0.131\rho_v h_{fg}.\left[\frac{\sigma g(\rho_l - \rho_v)}{\rho_v^2}\right]^{0.25} \tag{7}$$

Leinhard and Dhir [21] advanced Zuber correlation [20] by assuming the Helmholtz instability wavelength and Taylor instability wavelength to be equal.

$$q''_{CHF} = 0.149\rho_v h_{fg}.\left[\frac{\sigma g(\rho_l - \rho_v)}{\rho_v^2}\right]^{0.25} \tag{8}$$

These models were proposed for the stationary pool boiling conditions and the initial correlation was proposed by Katto's group [25–27] in 1980–1987. The model is based on the theory of Helmholtz instability between the vapour and liquid. They further assumed that the onset of nucleate boiling occurs when the heat from the heated surface exactly balances the latent heat of the liquid trapped in the liquid film layer and the ratio $\frac{\rho_v}{\rho_l}$ is very less than unity.

$$q''_{CHF} = 0.186G_l h_{fg}\left(\frac{\rho_v}{\rho_l}\right)^{0.559} We_l^{-0.264} \tag{9}$$

Where $We_l = G_l^2 \mathrm{L}/\rho_l\sigma$

Mudawar and Maddox [23] further modified the correlation and incorporated the geometrical effects and is applicable only when $0.0095 < \frac{\rho_v}{\rho_l} < 0.0102$

$$q''_{CHF} = 0.161G_l h_{fg}\left(\frac{\rho_v}{\rho_l}\right)^{15/23} We_l^{-8/23}\left(\frac{L}{d}\right)^{1/23} \tag{10}$$

Darr *et al* [24] proposed a correlation for maximum heat flux generated in a liquid nitrogen chilldown process. The proposed model was

$$q''_{CHF} = 0.527G_l h_{fg}(We)^{-0.2894} \tag{11}$$

The measured value and the predicted values of CHF are given in figure 7. A large variation is observed for Lieinhard and Dhir [21] and Zuber [20] correlations with a percentage deviation greater than 100%. This may be due to the different mechanisms in pool boiling and flow boiling conditions. In pool boiling criteria the surface is maintained at a constant temperature or constant heat flux whereas, in chilldown test the surface temperature is reduced due to the consumption of energy stored in the wall for boiling. Katto's correlation[25–27] and Darr's correlation [24] had a deviation of around 62% and 64%, whereas Mudawar and Maddox [23] correlation showed best agreement with an error of nearly 30%. All the correlations employed are only concerned about the fluid properties and have not considered any pipe wall properties.

Figure 8 provides a comparison of maximum heat fluxes in horizontal orientation in the present work and the data available from reported works, to the mass flux of the cryogen. It can be seen that under lower mass flux conditions the CHF observed in copper tubes are reduced to half, than observed in stainless steel tubes [16, 28] and had different CHF values among stainless steel tubes under similar mass flux conditions too.

This might be due to the variation in the thermal load of the systems. Under heavy insulated conditions, i.e., in

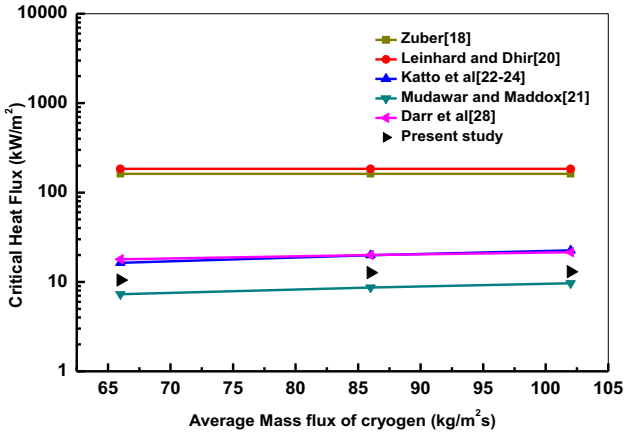

Figure 7. Predicted and measured values of CHF.

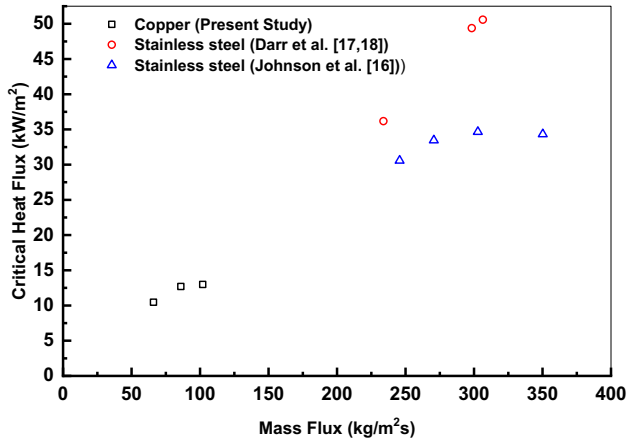

Figure 8. Variation of CHF with G.

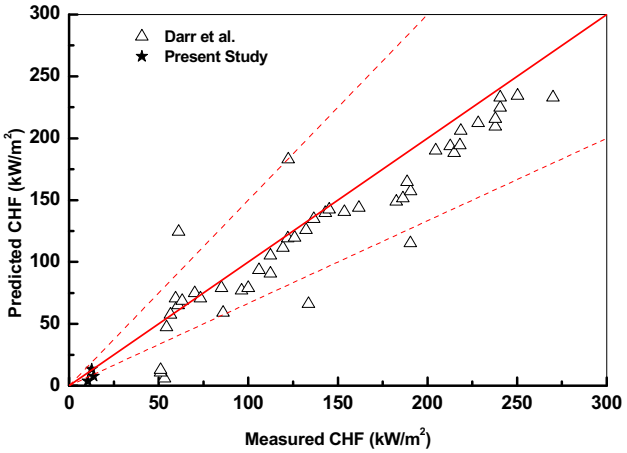

Figure 9. Variation of predicted and measured CHF.

the absence of any external heat loads, the thermal energy stored in the mass of the pipe wall is extracted during the chilldown procedure. The available thermal energy per unit volume of pipe wall could be provided as a product of thermal mass of the pipe wall with the maximum possible temperature difference $(M(T_i - T_{sat}))$. Thermal mass (M) can be calculated as the product of mass of test section and its specific heat (C_p) [16]. In the present study the thermal mass of the system was smaller than that of the previous studies and this could be the reason for the low CHF values under the present mass flux conditions. Under the absence of undercooling or any other external heat load, the initial wall temperature could be assumed to be equal to the ambient temperature and an empirical relation for CHF considering the thermal properties of the quenched wall could be developed. Data sets were obtained from the present study and previous reported works on short horizontal transfer tube. The obtained relation can be given as

$$q''_{CHF} = 1.54 \times 10^{-11}(M(T_i - T_{sat}))\left[\left(\frac{Re_l^{0.392}}{\sigma^{0.17}}\right)\frac{\mu_g^{0.503} h_{fg}^{0.206} G_l^{0.613}}{\rho_l^{0.047} D^{1.68}}\right] \quad (12)$$

Figure 9 shows the variation of predicted CHF to that of the measured CHF. More than 80% of the plotted data fit inside a 30% error limit of the correlation.

3.3 *Leidenfrost Temperature*

Leidenfrost temperature, also known as the rewetting temperature is the temperature at which liquid wets the wall surface. It is characterized by lowest heat flux in a film boiling curve. Zuber [20] provided a correlation for predicting the lowest heat flux for pool boiling experiments on flat plates as:

$$q''_{CHF} = 0.176\rho_v h_{fg}.\left[\frac{\sigma g(\rho_l - \rho_v)}{(\rho_l + \rho_v)^2}\right]^{0.25} \quad (13)$$

Berenson [22] modified Zuber's correlation [18] into:

$$q''_{CHF} = 0.091\rho_v h_{fg}.\left[\frac{\sigma g(\rho_l - \rho_v)}{(\rho_l + \rho_v)^2}\right]^{0.25} \quad (14)$$

This is one of the most commonly used expressions based on the observations in pool boiling over flat plates. Berenson [29] also provided an expression to predict the Leidenfrost temperature as:

$$T_{leid} - T_{sat} = 0.127\frac{\rho_v h_{fg}}{k_v}.\left[\frac{g(\rho_l - \rho_v)\mu_v}{(\rho_l + \rho_v)^2}\right]^{0.5} .\left[\frac{g_0\sigma}{g(\rho_l - \rho_v)}\right]^{0.33} \quad (15)$$

The computed values and measured minimum heat flux and Temperature are provided in table 2 and figure 10 respectively. Measured value was much smaller than the predicted value. The Zuber model [20] and Berenson model [22] were developed for pool boiling flow and thus find limited applicability in flow problems. These models were used by Schieffer *et al* [13] and found agreeable results with deviation of 25%. Hartwig *et al* [15] used the correlation to predict the Leidenfrost temperature and found agreeable results.

3.4 *Chilldown efficiency and Chilldown time*

Schieffer *et al* [13] coined the term Chilldown efficiency for transitional boiling regimes as the ratio between the amounts of measured energy from the pipe wall to what was capable of being absorbed by the fluid. Energy loss from the pipe wall can be calculated as the product of

Table 2. Predicted and measured values of minimum heat flux.

Mass flux (kg $(m^2s)^{-1}$)	Measured Minimum Heat flux in present study (kW. m^{-2})	Predicted Minimum Heat flux (kW. m^{-2})using models	
		Zuber [18]	Berenson [19]
102	1.2494		
86	1.1407	8.38	8.456
66	0.7078		

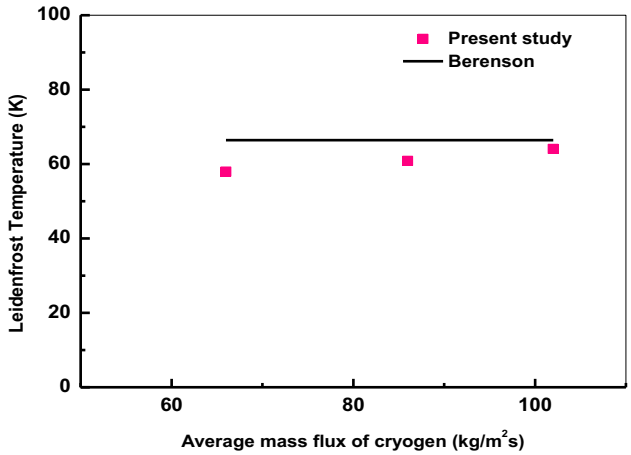

Figure 10. Predicted and measured Leidenfrost temperature.

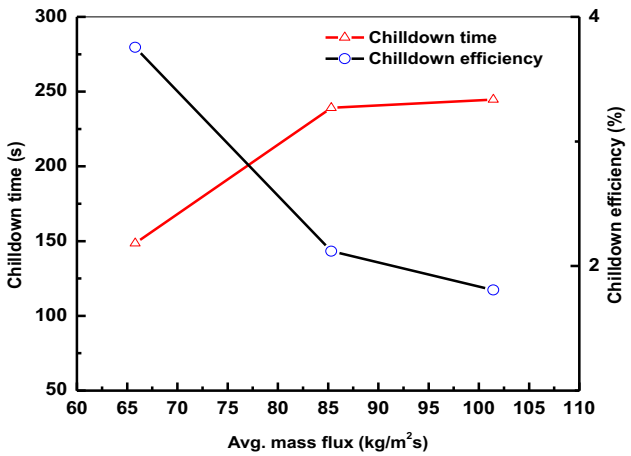

Figure 11. Variation of chilldown efficiency and chilldown time with mass flux.

thermal mass (M) and transient temperature difference $(T_{initial} - T_{final})$. Heat absorbed by the fluid can be given as the product of total mass of cryogen and latent heat of the fluid [13].

$$\eta = \frac{M\left(T_{initial} - T_{final}\right)}{mh_{fg}} \tag{16}$$

Chilldown time is taken as the time taken for the average outer wall temperature to reach steady value.

Figure 11 shows the variation of chilldown efficiency and chilldown time with average mass flux. It is observed that the mass flux has a significant influence on both chilldown efficiency and chilldown time.

4. Conclusions

This paper presents the results of an experimental study conducted on cryogenic chilldown of a copper transfer line. For analysing heat flow characteristics during chilldown process, the transient temperatures for different mass flux conditions were measured. It was identified that the chilldown characteristics of copper transfer lines with a simple insulation like Polyurethane foam were similar to that of previously published studies on steel transfer lines. It was identified that CHF obtained in chilldown of copper transfer lines under present mass flux conditions is 50% less than observed during previous studies with stainless steel transfer lines. Various correlations were employed to predict the CHF and Leidenfrost temperature. Katto's correlation and Darr's correlation had a deviation of around 62% and 64% whereas, Mudawar and Maddox correlation showed best agreement with an error about 30%. Correlations for predicting minimum heat flux show large deviation. The deviation of the predicted data may be due to the difference in flow patterns for pool boiling phenomena and film boiling phenomena. Moreover, the existing correlations are concentrated on the fluid characteristics without considering the pipe wall properties. Future work may be done to develop effective correlations that consider the properties of the pipe wall. Moreover the effect of various insulations and geometries on the test section needs to be explored.

Acknowledgement

The authors would like to thank Space Technology Laboratory in TKM College for engineering for setting up the experimental set-up. They would also like to express

gratitude for Technical Education Quality Improvement Programme Phase-II (TEQIP-II) promoted by National Project Implementation Unit, MHRD, Government of India for their support.

Nomenclature

C_p	Specific heat, J (kg. K)$^{-1}$
D	Inner diameter, m
L	Length, m
g	Acceleration due to gravity, m. s^{-2}
h	Heat transfer coefficient, W (m^2. K)$^{-1}$
h_{fg}	Latent heat of vaporization, J (kg. K)$^{-1}$
m	Mass of cryogen, kg
M	Thermal Mass, kJ. K^{-1}
G	Mass flux, kg (m^2.s)$^{-1}$
q''	Heat flux, W. m^{-2}
r	Radius, mm
T	Temperature, K
t	Time, s
ΔT	Wall super heat, K
z	Axial length, m
μ	Absolute viscosity, Pa. s
ρ	Density, kg. m^{-3}
σ	Surface tension coefficient, N. m^{-1}
α	Thermal Diffusivity m^2. s^{-1}
We	Weber Number

Abbreviations

OFHC	Oxygen Free High Conductivity Copper
PUF	Polyurethane foam
CHF	Critical heat flux

Subscripts

v	Vapor
l	Liquid
i	Inner surface of wall
o	Outer surface of wall
parasitic	Parasitic heat load
cond	Conductive heat load
conv	Convective heat load
rad	Radiative heat load
a	Axial length
sat	Saturation conditions
w	Wall
CHF	Critical heat flux

References

[1] Goswami T K 2010 Role of cryogenics in food processing and preservation. *Int. J. Food Eng.* 6: 2

[2] Davidge H 1981 Cryogenics in the food industry. *Cryogenics* 21: 287–290

[3] Burke J C, Byrnes W R, Post A H and Arthur F E R 1960 Pressurized cooldown of cryogenic transfer lines. *Adv. Cryog. Eng.* 45: 283–290

[4] Bronson, J C, Edeskuty F J, Fretwell J H, Hammel E F, Keller W E, Meier K L, Schuch A F and Willis W L 1962 Problems in cool-down of cryogenic systems. *Adv. Cryog. Eng.* 7: 198–205

[5] Chi J W H and Vetere A M 1964 Two-phase flow during transient boiling of hydrogen and determination of non equilibrium vapor fractions. *Adv. Cryog. Eng.* 9: 243–253

[6] Chi J W H 1965 Cooldown temperatures and cooldown time during mist flow. *Adv. Cryog. Eng.* 10: 330–340

[7] Srinivasan K, Seshagiri Rao V and Krishna Murthy M V 1974 Analytical and experimental investigation on cool-down of short cryogenic transfer lines. *Cryogenics* 14: 489–494

[8] Yuan K, Ji Y and Chung J N 2007 Cryogenic chilldown process under low flow rates. *Int. J. Heat Mass Transf.* 50: 4011–4022

[9] Yuan K, Ji Y and Chung J N 2009 Numerical modeling of cryogenic chilldown process in terrestrial gravity and microgravity. *Int. J. Heat Fluid Flow* 30: 44–53

[10] Jackson J, Liao J, Klausner J F and Mei R 2005 Transient heat transfer during cryogenic chilldown. *Heat Transfer* 2: 253–260

[11] Hu H, Chung J N and Amber S H 2012 An experimental study on flow patterns and heat transfer characteristics during cryogenic chilldown in a vertical pipe. *Cryogenics* 52: 268–277

[12] Jackson J, Liao J, Klausner J F and Mei R 2005 Transient heat transfer during cryogenic chilldown. In: *Proceedings of HT2005 ASME Summer Heat Transfer Conference 2005 ASME Summer Heat Transfer Conference.* 253–260

[13] Shaeffer R, Hu H and Chung J N 2013 An experimental study on liquid nitrogen pipe chilldown and heat transfer with pulse flows. *Int. J. Heat Mass Transf.* 67: 955–966

[14] Liu Y, Olewski T and Véchot L N 2015 Modeling of a cryogenic liquid pool boiling by CFD simulation. *J. Loss Prev. Process Ind.* 35: 125–134

[15] Hartwig J, Hu H, Styborski J and Chung J N 2015 Comparison of cryogenic flow boiling in liquid nitrogen and liquid hydrogen chilldown experiments. *Int. J. Heat Mass Transf.* 88: 662–673

[16] Johnson J and Shine S R 2015 Transient cryogenic chill down process in horizontal and inclined pipes. *Cryogenics* 71: 7–17

[17] Darr S R, Hu H and Glikin N 2016 An experimental study on terrestrial cryogenic tube chilldown II. Effect of flow direction with respect to gravity and new correlation set. *Int. J. Heat Mass Transf.* 103: 1243–1260

[18] Darr S R, Hu H and Glikin N G 2016 An experimental study on terrestrial cryogenic transfer line chilldown I. Effect of mass flux, equilibrium quality, and inlet subcooling. *Int. J. Heat Mass Transf.* 103: 1225–1242

[19] Jackson J K 2006 *Cryogenic two-phase flow during chilldown: Flow transition and nucelate boiling heat transfer*. Ph.D. Thesis University of Florida

[20] Zuber N 1958 On stability of boiling heat transfer. *Trans. ASME* 80: 711–720

[21] Lienhard J H and Dhir V K 1973 Hydrodynamic prediction of peak pool-boiling heat fluxes from finite bodies. *J. Heat Transf.* 95: 152–158

[22] Berenson P J 1961 Film-boiling heat transfer from a horizontal surface. *J. Heat Transf.* 351–356

[23] Mudawar I and Maddox D E 1990 Enhancement of critical heat flux from high power microelectronic heat sources in a flow channel. *J. Electron. Packag.* 112: 241–248

[24] Darr S R, Hu H, Shaeffer R, Chung J, Hartwig J W and Majumdar A K 2015 Numerical simulation of the liquid nitrogen chilldown of a vertical tube. In: *53rd AIAA Aerospace Sciences Meeting* 1–13

[25] Katto Y and Ohno H 1984 An improved version of the generalized correlation of critical heat flux for the forced convective boiling in uniformly heated vertical tubes. *Int. J. Heat Mass Transf.* 27: 1641–1648

[26] Katto Y 1978 A generalized correlation of critical heat flux for the forced convection boiling in vertical uniformly heated round tubes-a supplementary report. *Int. J. Heat Mass Transf.* 21:1527–1542

[27] Katto Y and Kurata C 1980 Critical heat flux of saturated convective boiling on uniformly heated plates in a parallel flow. *Int. J. Multiph. Flow* 6: 575–582

[28] Jin L, Park C, Cho H, Lee C and Jeong S 2016 Experimental investigation on chill-down process of cryogenic flow line. *Cryogenics*79: 96–105

[29] Berenson P J 1960 Transition boiling heat transfer from a horizontal surface. In: *M.LT. Heat Transfer Laboratory Technical Report* 17